Modelling of optical synchronization of chaotic external cavity VCSELs

P.S.Spencer*, Claudio.R.Mirasso+, P.Colet++ and K.Alan Shore*

(∗) University of Wales, Bangor, School of Electronic Engineering and Computer Systems, Bangor. LL57 1UT, Wales, UK.

(+) Department de Física, Universitat de les Illes Balears, E-07071 Palma de Mallorca, España.

(++) Instituto Mediterraneo de Estudiados Avanzados, IMEDEA, (CSIC-UIB) E-07071 Palma de Mallorca, España.

Abstract

The performance of a master-slave configuration for effecting the synchronization of chaotic VCSELs is studied using numerical simulations. The dynamical evolution of optically coupled VCSELs is examined using a travelling wave model which is valid in the strong optical feedback regime. It is shown that the proposed configuration is capable of effecting synchronization in a robust manner. The opportunity for exploiting synchronized chaos in secure optical communication systems is indicated.

1 Introduction

Advances in the understanding of nonlinear dynamical systems have led to interest in developing practical applications for chaotic dynamics in a number of disciplines including laser physics, medicine and communications. These efforts received a significant stimulus following the publication of a chaos control technique by Ott, Grebogi, and Yorke (OGY) [1] which led to several demonstrations of the control of chaotic dynamics in a number of laser systems [2-4]. Attention is drawn, in particular, to studies of the control of chaotic dynamics in external cavity edge-emitting laser diodes exhibiting coherence collapse [5-12].

Interest in controlling semiconductor laser dynamics has been stimulated primarily by the possibilities for achieving secure communication systems which exploit the properties of chaotic dynamical systems [13]. Chaotic communications may, in particular, be effected by mixing the message signal with the output from a chaotic transmitter and then recovering the message from the received transmitted chaos using the concept of chaos synchronization [14]. An efficient algorithm for improving the locking rate between receiver and transmitter in such systems has been reported previously [15].

The use of synchronized chaotic lasers was previously proposed as an approach to effecting data encryption [16]. The feasibility of optical injection-locking techniques for reciprocal synchronization of two distant chaotic laser diodes has been considered [17]. Very recent experimental results have successfully shown it is possible encoded and decoded a signal using chaotic encryption, [18]. The experiment used a configuration containing two synchronized edge-emitting laser diodes. Other schemes for synchronizing chaotic laser diodes have also been examined [19]. Conversely, chaos control techniques are also of interest from a conventional optical communications systems viewpoint since there they may be used for ensuring immunity to coherence collapse [20]. Reviews of the relevant effects and further references thereon may be found in [21,22].

It has been shown experimentally that, despite their high facet reflectivities [23], VCSELs are sensitive to optical feedback effects. This has been interpreted in terms of the similarity between photon lifetimes in edge-emitting laser diodes and VCSELs [24]. Furthermore, it has been shown recently using a travelling wave model [25] that VCSELs subject to strong optical feedback can exhibit chaotic dynamics over a wide range of operating currents [26]. The synchronization system to be analysed here assumes a VCSEL master-slave configuration similar to that previously suggested for a edge-emitting laser diode based scheme, [27]. The aim of the present contribution is to demonstrate, via numerical simulations, that synchronization of VCSEL chaotic dynamics can be effected in a robust manner. The simulations indicate that synchronization is attainable under experimentally achievable conditions, and that the synchronization is not overly sensitive to small fluctuations in parameter values. This is a somewhat surprising result because the very high laser facet reflectivities of VCSELs drastically limits the amount of injected signal that can be coupled into the slave laser, and would thus also be expected to place tight limits on the range of parameter values allowed before synchronization is lost. It is also by no means clear that the much reduced coupling in VCSELs would be sufficient to allow synchronization in any case. The result for the VCSEL based master-slave synchronization scheme analysed here open the attractive possibility of using VCSELs as sources in chaotic optical receiver / transmitter modules.

2 Model

Attention is given to the case of two identical VCSELs which are optically coupled. It is supposed that optical isolation is arranged so that the output of one device (the master laser) can be used to influence that of the second laser (the slave laser) but not vice versa. Both lasers are assumed to be operating in a chaotic regime. Such chaos can be obtained in a number of ways but in the present work it is assumed that the lasers are driven into chaos due to optical feedback from an external reflector. Even though the devices are taken to be identical, when the lasers operate independently their (chaotic) outputs would be expected to be different. In this work it will be shown that conditions for synchronizing the chaotic outputs of the lasers can be identified. Moreover an optimisation is performed of the regimes in which such synchronized chaos can be obtained.

The analysis has been undertaken using a modification of travelling-wave model which is valid in the present optical feedback regime [24] the analysis takes into account the effect of optical injection from the master laser on the slave dynamics.

For convenience the main elements of the iterative scheme are described here. The iterative model is based on a perturbation approach. The unperturbed state is assumed to be that of a solitary laser and the perturbation is provided by optical feedback. The slowly varying envelope function of the field, A, is calculated in steps of the laser diode's internal round-trip delay, τ_{in}. The field equations of the master, $A_m(t)$, and slave, $A_s(t)$, lasers are given below,

$$A_m(t+\tau_{in}) = \frac{e^{G(1+i\alpha)}}{r_2}\left[r_2 A_m(t) + r_3(1-r_2)\sum_{q=1}^{\infty}(-r_2 r_3)^{q-1} A_m(t-q\tau)e^{-iq\Phi_E}\right] \quad (1)$$

$$A_s(t+\tau_{in}) = \frac{e^{G(1+i\alpha)}}{r_2}\left[r_2 A_s(t) + r_3(1-r_2)\sum_{q=1}^{\infty}(-r_2 r_3)^{q-1} A_s(t-q\tau)e^{-iq\Phi_E} + \beta A_m(t)e^{i\Delta\omega t}\right]$$

where $\Phi_E = \omega_0\tau$ is the accumulated phase in the external cavity, $\omega_0 = 2\pi\, c/\lambda_0$ is the angular frequency of the solitary laser, and $G = g_n\,(n - n_t)\,\tau_{in}/2$. The summation terms in eqn(1) accounts for multiple reflections and includes a phase term, Φ_E that describes any phase shift that may develop between the field in the laser and the field in the external cavity. The equation for the slave laser includes an additional term that accounts for the optical injection from the master laser. This term contains a phase term that allows for frequency detuning between the two lasers, $\Delta\omega = \omega_m - \omega_s$; however, in the present work zero detuning has been assumed. For simplicity we have neglected spontaneous emission noise in eqn(1). This is justified as the deterministic characteristics are being investigated here. Also previous reports on various aspects of the coherence collapse regime have shown that spontaneous emission has primarily a quantitative effect on the dynamics, and does not change the qualitative behaviour, [28,29].

The carrier number equation is incorporated into an iterative scheme by using a second-order Taylor expansion,

$$n_j(t+\tau_{in}) \simeq n_j(t) + \tau_{in}\frac{d\,n_j}{d\,t} + \frac{\tau_{in}^2}{2}\frac{d^2\,n_j}{d\,t^2} \quad (2)$$

The first-order derivative is simply the well known standard carrier rate equation and the second order is found by differentiation,

$$\frac{d\,n_j(t)}{d\,t} = \frac{I(t)}{e} - \frac{n_j(t)}{\tau_e} - g_n(n-n_o)\,S_j(t) \quad (3)$$

In these equations $S_j(t) = |A_j(t)|^2$ is the photon number inside the laser cavity. Where $j = m$ or s to denote the master or slave laser respectively. Numerical values of parameters used in eqn(1)-eqn(3) are given in Table(1).

Typical parameters for electrically driven VCSELs have been used as given in Table(1). Attention is focussed on the influence of the laser driver current; the coupling between the lasers and the strength of the optical feedback. In particular attention will be given to cases of relatively low optical feedback -corresponding to an external mirror (power) reflectivity of 1% and a relatively high external reflectivity of 50%.

3 Chaotic regimes of VCSELs subject to strong optical feedback

The essential prerequisite for the proposed scheme of synchronization is that the VCSELs are, in fact operating in a chaotic regime when subject to conventional optical feedback. This is confirmed via the simulations which are presented in figure(1). The typical time traces for two external reflectivity $R_{ext} = 1\%$ and $R_{ext} = 50\%$ ($R_{ext} = r_3^2$) used in the subsequent analysis are shown in figure(1a). The large irregular fluctuations in the photon number, which are synonymous with chaotic regime, are clearly visible. The accompanying increase in the spectral width (coherence collapse) is shown in figure(1b). All the parameter used in the simulations are listed in Table(1). Further discussion of coherence collapse in VCSELs can be found in [25].

4 Synchronized Chaos

4.1 Characterisation of synchronization procedure

To illustrate the effectiveness of the present scheme we show, in figure(2), calculated photon numbers as a function of increased optical coupling for master and slave lasers biased at 4 times the stand-alone threshold current and subjected to feedback from a high external reflectivity mirror. In the case of very low optical coupling (figure(2a)) the correlation between the outputs of the master and slave lasers is rather poor. As the coupling is increased (although remaining at practically-attainable values) towards an optimum value (figure(2b)) the correlation becomes significantly improved and it may be said that the lasers are synchronized. Further increase in the coupling coefficient is seen to destroy the synchronization. (figure(2c)). In the first case it is apparent that the signal from the master laser is too weak to effect the synchronization whilst at the largest value the behaviour of the slave is too strongly affected by the master laser.

It has been found that all optical coupling values above the optimum case have the same characteristic 'lobed' synchronization pattern, figure(2c), where the largest excursions from the mean value are seen when the master laser is at high power. The larger the optical coupling the more pronounced this 'lobed' synchronization pattern becomes. This indicates that optical pumping is dominating the behaviour of the slave laser when the output power of the master laser is high. This large injected optical signal either saturates or dramatically increases the output power of the slave laser. However, when the output power of the master laser is low, synchronization can be achieved. Thus, for high coupling cases synchronization is not totally lost but becomes dependent on the absolute output power of the master laser. That is, synchronization is obtained when master laser output power is small, but is lost when the output is high.

In contrast for very weak optical injection all synchronization is lost and this is reflected in the synchronization pattern which is uniformally populated over all power values. In other

words, for any given master laser power, the slave laser is equally likely to have any output power, since the two devices are uncorrelated. The same qualitative behaviour is observed for the case of low external reflectivity.

In order to characterise the degree of synchronization in the numerical simulations we first need to define what we mean by 'perfect' synchronization and then use this as a reference.

In theory perfect synchronization is obtained in the limit of a vanishingly small (but nonzero) optical injection into the slave laser, that is $\beta \to 0$. In this case the chaotic dynamics are synchronized and the output powers of both lasers are identical. Hence a least squares linear fit of the slave output power versus the master output power would give a 45° straight line, with slope $m = 1$ and standard deviation $\sigma = 0$.

In practice the master and slave lasers can never be perfectly synchronized and thus the standard deviation is always a small finite number. Similarly since β is not generally vanishingly small the injected signal from the master laser not only synchronizes, but also optically pumps the slave laser, thus the output power of the slave is always slightly higher than that of the master. So in practice the gradient is generally greater then unity. This is clearly evident in figure(2). In figure(2a) where the coupling is below the optimum values, the slope and standard deviation are $m = 1.15$ and $\sigma = 3.0 \times 10^{-3}$, while at optimum coupling, figure(2b), the slope is slightly higher $m = 1.3$, due to increased optical pumping, but the standard deviation is almost ten times smaller $\sigma = 0.4 \times 10^{-3}$. If the coupling is increased above the optimum value, the optically pumping effect becomes more significant than the synchronization influence of the injected optical signal. Consequently both the slope $m = 2.4$ and standard deviation $\sigma = 1.1 \times 10^{-3}$. increase.

It is clear from the above that the standard deviation σ can be used as a convenient measure of the degree of synchronization between the master and slave lasers, (where it understood that perfect synchronization is obtained when $\sigma = 0$). The effect that the external reflectivity, drive current and coupling coefficient have on the quality of the synchronization will now be investigated. These three parameter are the most experimentally amenable to alteration, and so the sensitivity of the synchronization to fluctuations in these parameters, and the interplay between them, will help determine whether synchronization is experimentally feasible. The outcome of such calculations are stated below.

The existence of an optimum coupling coefficient for a given external reflectivity and drive current can clearly be seen in figure(3). Regardless of the exact values of the external reflectivity and drive current the optimum coupling coefficient is always within the range $0.01 < \beta < 0.05$. Figure(3) also shows that the range of values of β over which synchronization can be achieved decreases with current irrespective of r_3. The same qualitative trends are seen for both low and high external reflectivities, (fig(3a) and fig(3b) respectively), highlighting the relatively weak effect which the external reflectivity has on the degree of synchronization. The only noticeable difference between figure(3a) and figure(3b) is the more abrupt change seen when moving from unsynchronized to synchronized behaviour in the low external reflectivity case. At no value of the coupling coefficient was the slave laser forced out of the coherence collapse regime, and the spectrum of the slave laser and master laser were almost indistinguishable; reflecting the fact that the two laser were operating around the same attractor in the carrier - photon density phase space(this point is discussed further in the next section).

Attention is now given to the dependence of synchronization on the laser drive current. Figure(4) shows the effect of drive current for two external reflectivity and a range of coupling coefficients around the optimum value, shown in figure(2). The results demonstrate the existence of a range of bias currents over which synchronization can be achieved almost independently

of the strength of the external feedback, figure(4b). However, for coupling coefficients away from the optimum value the synchronization is more effective for lower values of the external reflectivity, figures(4a,c).

The effect that the external mirror reflectivity has on the synchronization process has also been examined. In figure(5) the dependence of σ on the external reflectivity, r_3, is shown for different values of the laser drive current and as a function of the coupling efficiency. It is seen that for the range of coupling efficiencies for which synchronization is obtained the standard deviation remains small and almost constant independent of the external reflectivity. As the drive current is increased the range of the coupling efficiency for which synchronisation is achieved becomes narrower. This indicates that when the laser is driven well above threshold the chaotic dynamics becomes less sensitive to external influence. Nevertheless an acceptable range of coupling efficiencies to allow synchronization is still obtained.

4.2 Phase Plane Representation of Synchronized Dynamics

The above results demonstrate the general effectiveness of the proposed procedure. It is instructive also to examine more carefully the effect of the synchronization on the master and slave dynamics. It is found, in this way, that the synchronization process is effective in, perhaps, a surprisingly exact way. Results justifying this assertion are given in figures(6,7) for the cases of low and high external mirror reflectivity. In figure(6a) the photon number / normalised carrier inversion phase-plane representation of the chaotic master laser is shown. In figure(6b) through figure(6d) the corresponding phase-plane portraits for the slave laser are shown. It is seen that when the optimum condition for synchronization is reached the dynamics of the slave replicates, almost in every detail, that of the master laser. Discernible differences in the phase portrait appear when the conditions for synchronization are not met. As the coupling between the lasers is changed it is seen that there is a shift to lower carrier densities/higher photon numbers. This is consistent with the change in carrier density arising due to the increased optical power in the slave laser as a consequence of increased optical coupling. The same qualitative features are seen in figure(7) which represents the master and slave dynamics for the case of high external mirror reflectivity. Again a quite remarkable similarity in the phase plane portraits of the master and slave is obtained when optimum conditions for synchronization are met.

5 Conclusion

In conclusion, it has been numerically shown that two chaotic VCSELs can be synchronized via optical coupling under appropriate conditions. The VCSELs were driven into the chaotic regime by external optical feedback, and as intuitively expected, the higher the external reflectivity the more chaotic the output power dynamics. For the higher external reflectivity cases multiple reflection effects within the external cavity become important and these effects are fully accounted for in the model. In all the cases investigated synchronization has been observed over a range of values of the coupling parameter. This range is large enough to ensure that synchronization is attainable within experimental tolerances.

The degree of synchronization has been studied as a function of the three main experimentally adjustable parameters: drive current, external reflectivity, and coupling coefficient. These numerical simulation revealed the following trends. (1) An optimum coupling coefficient exists for any given reflectivity and drive current. (2) There is a relativity weak dependence on the external reflectivity, but the lower the external reflectivity the better the synchronization. (3)

For a given coupling coefficient there is a range of drive current over which the degree of synchronization is roughly constant. In all the cases studied the best synchronization was always obtained for a coupling coefficient within the range $0.01 < \beta < 0.05$.

The capability outlined open the possibility of using these devices in compact modules to implement secure optical communications based upon chaotic data encryption.

Acknowledgements

This work was undertaken with support from the British Council/ Ministerio de Educacion y Cultura de Espana, Acciones Integradas OCCULT project. The work of P.S.Spencer and K.A.Shore was supported by the UK EPSRC grants GR/K80136 and GR/K83625 respectively. The work of C.Mirasso and P.Colet is also supported by the projects TIC97-0420 and TIC95/0563 of the Commisión Interministerial de Ciencia y Tecnología CICYT (Spain).

References

[1] E.Ott, C.Greboggi and J.A.Yorke, "Controlling chaos " Phys. Rev. Lett., 64, 1196-1199, (1990).

[2] R.Roy, T.W.Murphy, T.D.Maier, Z.Gills, E.R.Hunt, "Dynamical control of a chaotic laser - experimental stabilisation of a globally coupled system," Phys. Rev. Lett., 68, 1259-1261, (1992).

[3] S.Bielawski, M.Bouazaoui, D.Derosier, P.Glorieux, "Stabilization and characterization of unstable steady states in a laser," Phys. Rev. A,47, 3276-3279, (1993).

[4] S.Bielawski, M.Bouazaoui, D.Derosier, P.Glorieux, "Controlling unstable periodic orbits by delayed continuous feedback," Phys. Rev. E, 49, R971-R973, (1994).

[5] G.R. Gray, A.T.Ryan, G.P.Agrawal, and E.C.Gage, "Optical feedback induced chaos and its control in semiconductor lasers", Chaos in Optics, SPIE Proc. Vol.2039, ed. R.Roy, pp. 45-57, (1993).

[6] Y.Liu, and J.Ohtsubo, "Experimental control of chaos in a laser diode interferometer with delayed feedback," Opt. Lett, 19, No.7, 448-450, (1994).

[7] A.T.Ryan, G.P.Agrawal, G.R.Gray, and E.C. Gage, "Optical feedback induced chaos and its control in semiconductor lasers", IEEE J.Quantum Electron., 30, 668-679, (1994).

[8] N.Watanabe and K.Karaki, "Inducing periodic oscillations from chaotic oscillations of a compound-cavity laser diode with sinusoidally modulated drive", Opt. Letts., 20, 725-727, (1995).

[9] Y.Liu, N.Kikuchi and J.Ohtsubo, "Controlling dynamical behaviour of a semiconductor laser with external optical feedback", Phys. Rev. E, 51, R2697-R2700, (1995).

[10] N.Kikuchi, Y.Liu and J.Ohtsubo, "Chaos control and noise suppression in external cavity semiconductor lasers", IEEE J. Quantum Electronics, 33, 56-65, (1997).

[11] S.I.Turovets, J.Dellunde and K.A.Shore, "Selective excitation of periodic dynamics in external-cavity laser diodes", Electron. Lett., 32, 42-43, (1996).

[12] S.I.Turovets, J.Dellunde and K.A.Shore, "Nonlinear dynamics of a laser diode subjected to both optical and electronic feedback", J. Optical Society of America B, 14, 200-208, (1997).

[13] S.Hayes, C.Greboggi and E.Ott, "Communicating with Chaos", Phys. Rev. Lett., 70, 3031-3034, (1993).

[14] K.M.Cuomo and A.V.Oppenheim, "Circuit implementation of synchronised chaos with applications in communications", Phys. Rev. Letts., 71, 65-68, (1993).

[15] K.A.Shore and D.T.Wright, "Improved synchronisation algorithm for secure communications systems using chaotic encryption", Electron. Lett, 30, 1203-1204, (1994).

[16] P.Colet and R.Roy, "Digital communication with synchronized chaotic lasers", Optics Letts., 19, 2056-2058, (1994).

[17] C.R.Mirasso, P.Colet and P.Garcia-Fernandez, "Synchronization of Chaotic Semiconductor Lasers: Application to Encoded Communications", IEEE, Photonics Tech. Lett., 8, 299-301, (1996).

[18] J.P.Goedgebuer, L.Larger and H.Porte, " Optical Cryptosystem Based on Synchronization of Hyperchaos Generated by a Delayed Feedback Tunable Laser Diode," Phys. Rev. Lett., **80**, 2249-2252, (1998).

[19] V.Annovazzi-Lodi, S.Donati, and A.Scire, "Synchronisation of chaotic injected laser systems and its application to optical cryptography", IEEE J. Quant. Electron., 32, 953-959, (1996).

[20] J.Wieland, C.R.Mirasso and D.Lenstra, "Prevention of coherence collapse in diode lasers by dynamic targetting", Optics Lett., 22, 469-471, (1997).

[21] G.H.M.van Tartwijk and D. Lenstra, "Semiconductor lasers with optical injection and feedback", Quantum. Semiclass. Opt., 7, 87-143, (1995).

[22] K.Petermann, "External Optical Feedback Phenomena in Semiconductor Lasers", IEEE J. Selected Topics in Quantum Electronics, 1, 480-489, (1995).

[23] S.Jhiang, Z.Pan,M.Dagenais, R.A.Morgan and K.Kojima "Influence of external optical feedback on threshold and spectral characteristics of VCSELs", IEEE Phot. Tech. Letts., 6, 34-36, (1994).

[24] L.N.Langley and K.A.Shore, "The effect of optical feedback on noise properties of VCSELs", IEE Proc., 144, 34-38, (1997).

[25] L.N.Langley, J.Mork and K.A.Shore, "Dynamics and noise properties of semiconductor lasers subject to strong optical feedback", Optics Letts., 19, 2137-2139, (1994).

[26] P.S.Spencer, C.R.Mirasso and K.A.Shore, "Strong optical feedback effects on the dynamics of VCSELs", IEEE Phot. Tech. Lett., **10**, 191-193, (1998).

[27] V. Annovazzi-Lodi, S.Donati and A.Scire, "Synchronisation of Chaotic Injected-Laser Systems and Its Application to Optical Cryptography," IEEE J. Quantum. Electron., **32**, 953-959, (1995).

[28] G.H.M van Tartwijk, A.M.Levine and D.Lenstra, "Sisyphus Effect in Semiconductor lasers with Optical Feedback," IEEE J. Select. Top. Quant. Electron., **1**, 466-474, (1995).

[29] S.I.Turovets, A.Valle and K.A.Shore, "Effects of noise on the turn on dynamics of a modulated class-B laser in the generalized multistability domain," Phys. Rev. A., **55**, 2426-2434, (1997).

Figure and Table Captions

- **Figure(1):** (a) Chaotic dynamics in external cavity VCSELs for external reflectivity for 1% and 50%. (b) The frequency spectrum for each case. In both (a) and (b) the $R_{ext} = 50\%$ case has been displaced vertically for clarity.

- **Figure(2):** Slave laser (SL) photon number vs Master laser (ML) photon number for optical coupling of: a) 1%, b) 2%, c) 7%. The straight lines denote the linear least squares fit for each case. In all cases the external reflectivity was $R_{ext} = 50\%$, and the injected was $I = 4.0 I_{th}$.

- **Figure(3):** Standard deviation from the least squares fit vs Coupling coefficient. Three normalised drive currents of 2.0 (circles), 4.0 (triangles), and 6.0 (rhombus), have been used for the two external reflectivities considered of a) $R_{ext} = 1\%$, b) $R_{ext} = 50\%$.

- **Figure(4):** Standard deviation from the least squares fit vs normalised injection current. Boxes correspond to an external reflectivity of 50 % and circles correspond to an external reflectivity of 1%, optical coupling of; a) 1%, b) 2%, c) 5%.

- **Figure(5):** Standard deviation from the least squares fit vs external reflectivity, r_3, for optical coupling of 1% (circles); 3% (squares) and 5% (stars) and normalised injection current; a) 2.0, b) 4.0, c) 6.0.

- **Figure(6):** Photon number- normalised inversion density phase plane dynamics for an external reflectivity of 1%: Master laser a) and Slave laser with optical coupling of b) $\beta = 1\%$, c) $\beta = 2\%$, d)$\beta = 5\%$.

- **Figure(7):** Photon number-normalised inversion density phase plane dynamics for an external reflectivity of 50%: Master laser a) and Slave laser with optical coupling of b) $\beta = 1\%$, c) $\beta = 2\%$, d) $\beta = 5\%$.

- **Table(1):** Description and values of laser parameters.

Symbol	Description	Value
τ_e	Carrier lifetime	2.0 ns
τ_{ph}	Photon Lifetime	2.7 ps
g_n	Differential Gain	6.52×10^{-9} ps^{-1}
n_0	Transparency Carrier Number	5.2×10^{7}
I_t	Threshold Current	8.7 mA
τ_{in}	Laser Round-Trip Time	0.15 ps
τ	External Round-Trip Time	1.0 ns
α	Linewidth Enhancement Factor	3.0
n_g	Group refractive index	4.0
λ_0	Wavelength of the Solitary Laser	870 nm
r_2	Laser Facet Field Reflectivity	0.995
e	Electronic Charge	1.602×10^{-19} coul

Table 1:

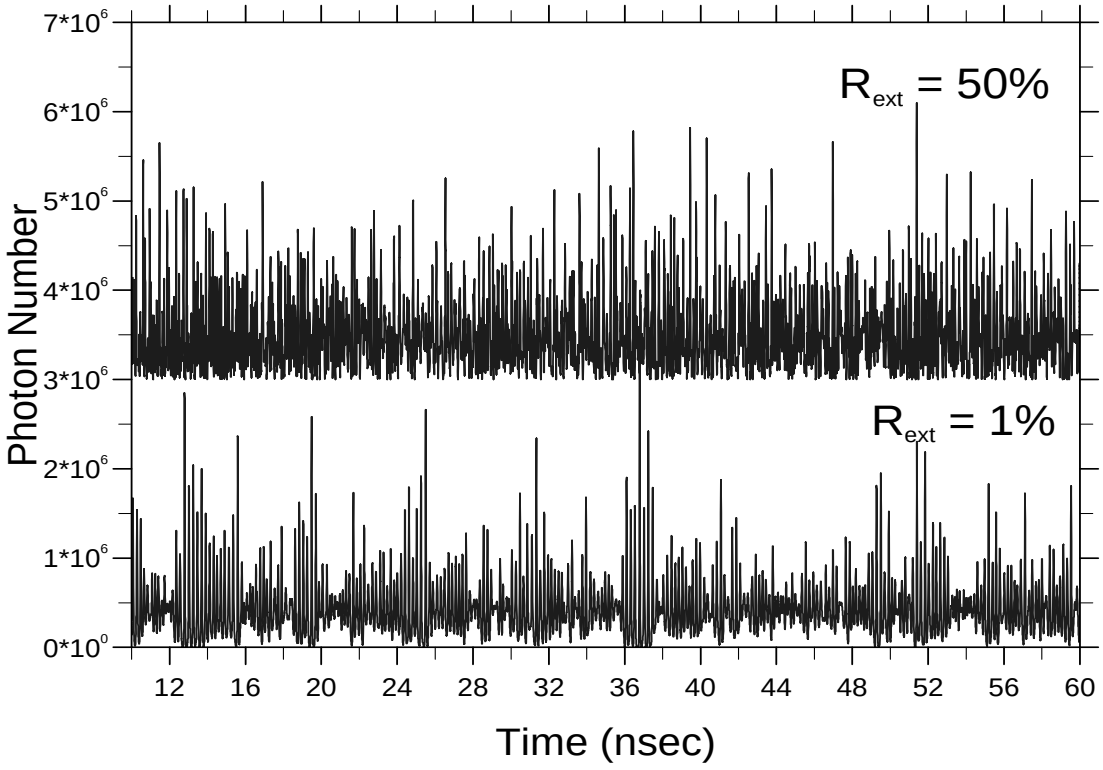
Photon Number
7*10^6
6*10^6
5*10^6
4*10^6
3*10^6
2*10^6
1*10^6
0*10^0
R_ext = 50%
R_ext = 1%
12
16
20
24
28
32
36
40
44
48
52
56
60
Time (nsec)

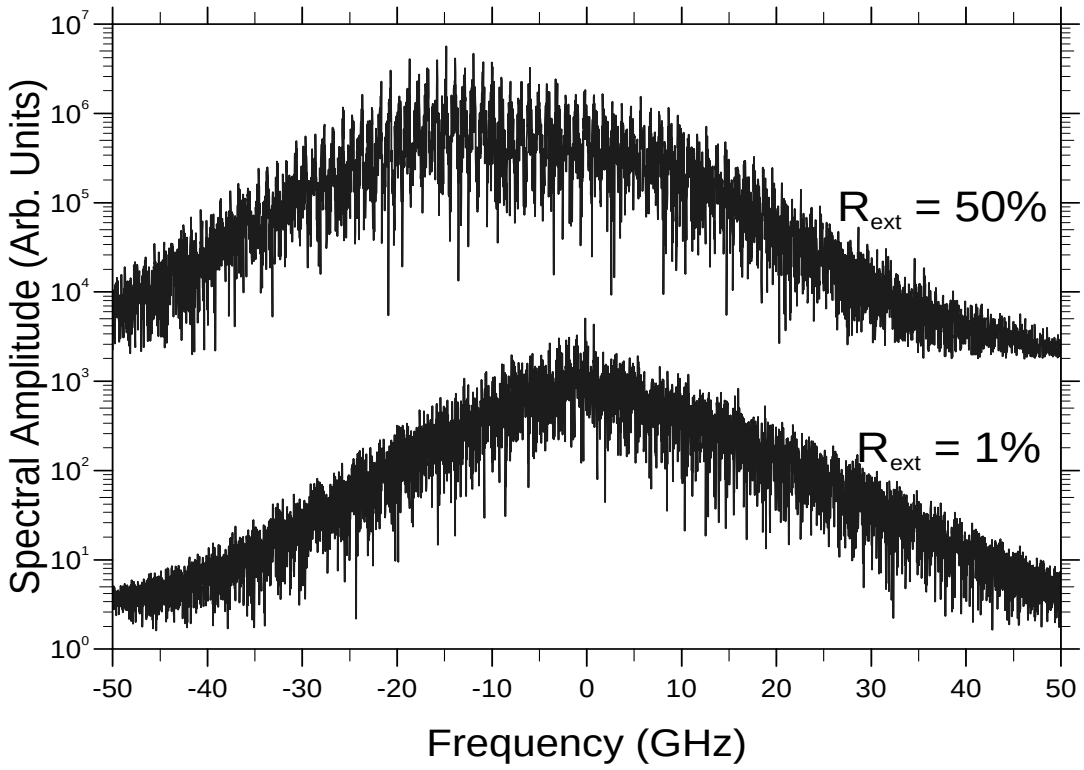
Spectral Amplitude (Arb. Units)
10^7
10^6
10^5
10^4
10^3
10^2
10^1
10^0
R_ext = 50%
R_ext = 1%
-50
-40
-30
-20
-10
0
10
20
30
40
50
Frequency (GHz)

Figure 1:

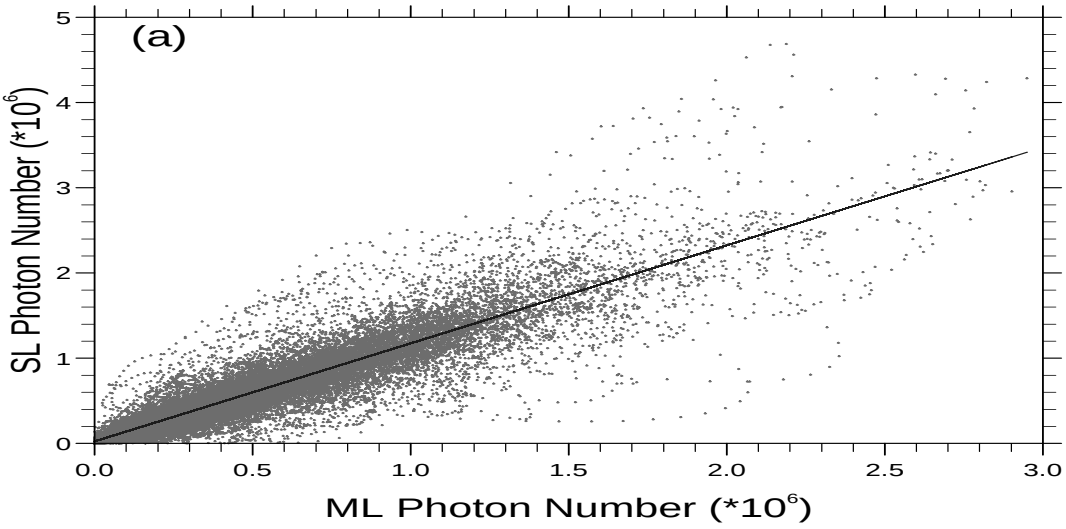
(a)
SL Photon Number (*10^6)
ML Photon Number (*10^6)
0
1
2
3
4
5
0.0
0.5
1.0
1.5
2.0
2.5
3.0

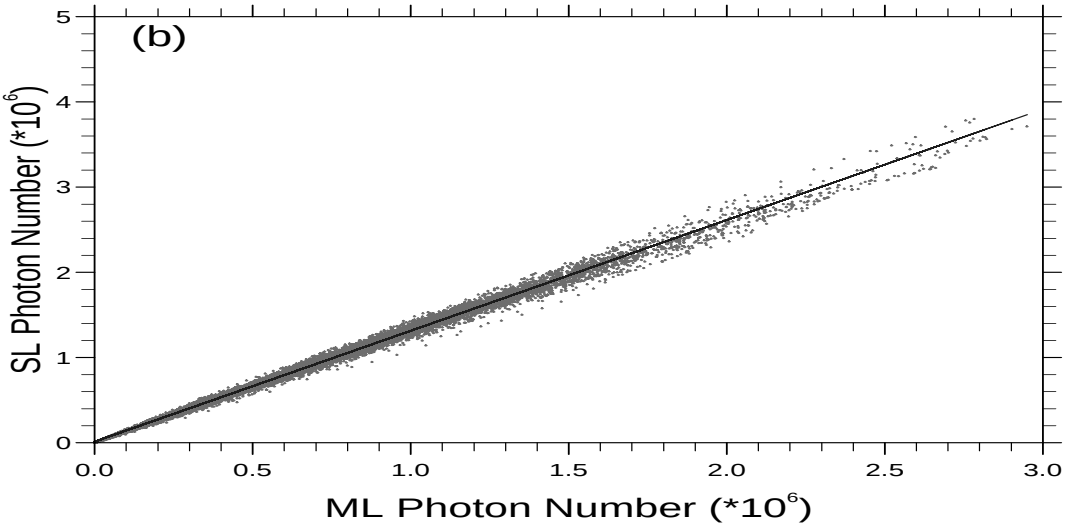
(b)
SL Photon Number (*10^6)
ML Photon Number (*10^6)
0
1
2
3
4
5
0.0
0.5
1.0
1.5
2.0
2.5
3.0

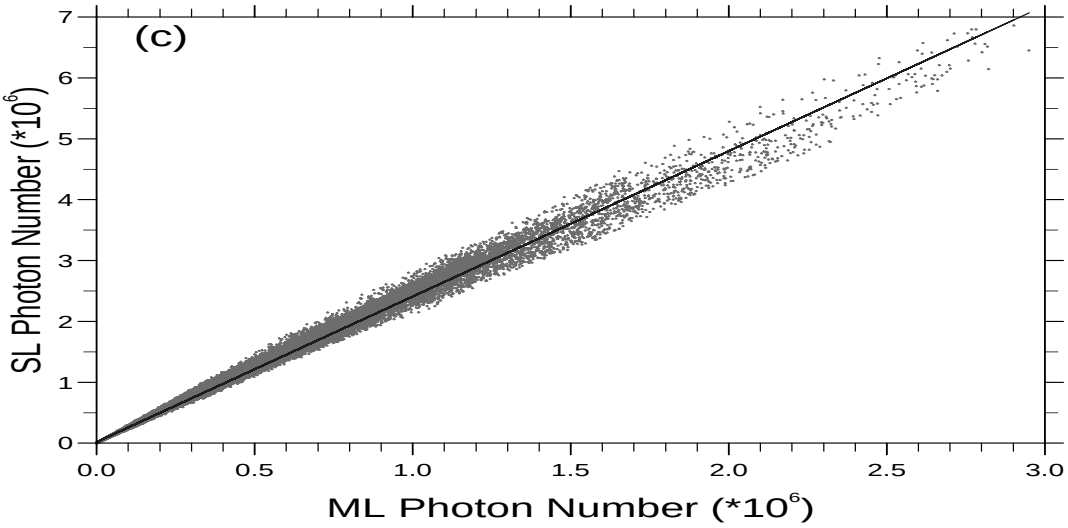
(c)
SL Photon Number (*10^6)
ML Photon Number (*10^6)
0
1
2
3
4
5
6
7
0.0
0.5
1.0
1.5
2.0
2.5
3.0

Figure 2:

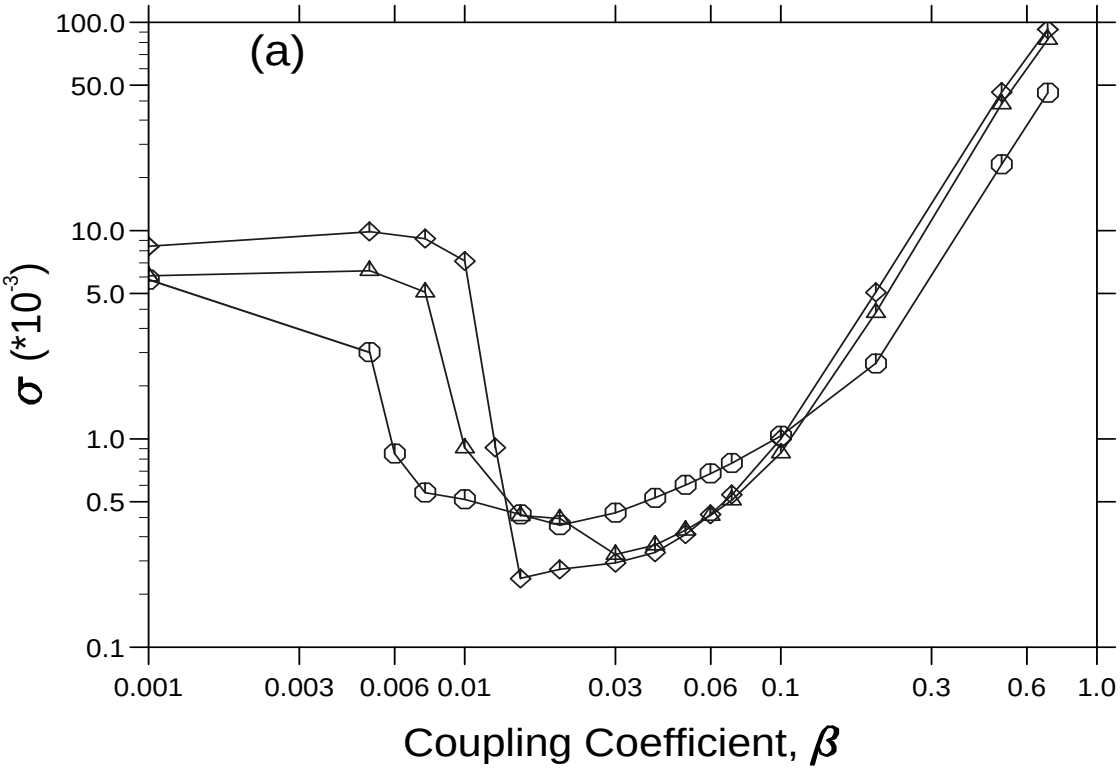
(a)
100.0
50.0
10.0
5.0
1.0
0.5
0.1
σ (*10^-3)
0.001
0.003
0.006
0.01
0.03
0.06
0.1
0.3
0.6
1.0
Coupling Coefficient, β

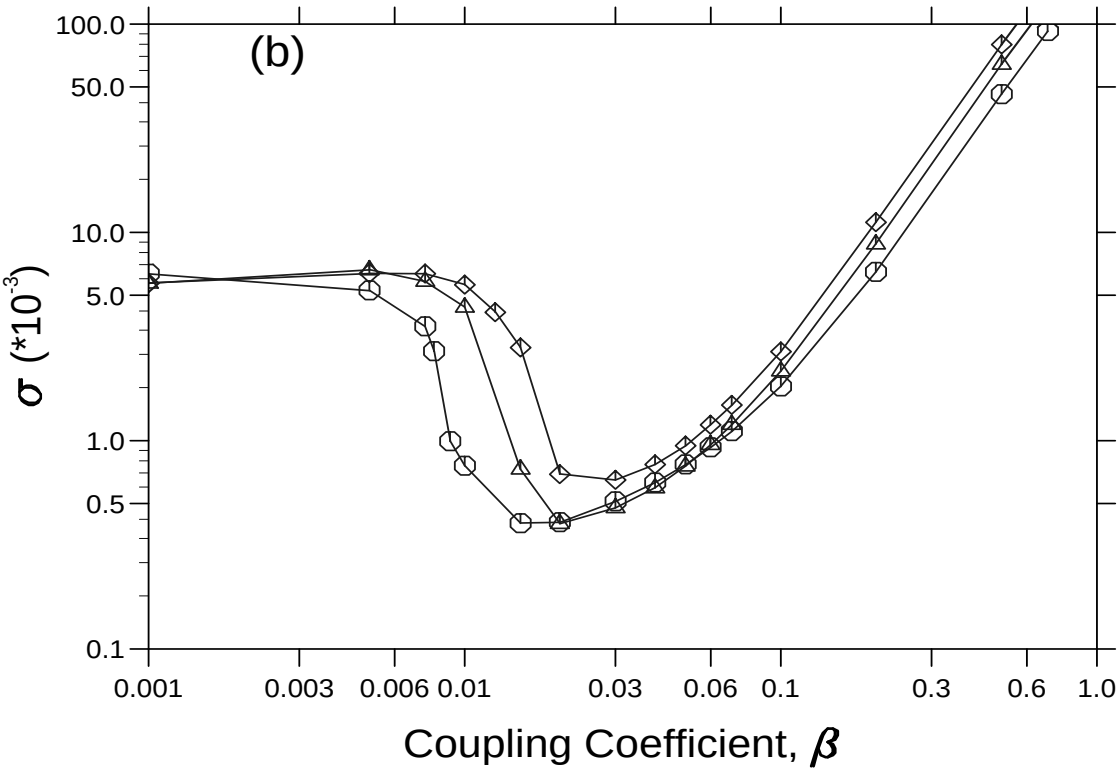
(b)
100.0
50.0
10.0
5.0
1.0
0.5
0.1
σ (*10^-3)
0.001
0.003
0.006
0.01
0.03
0.06
0.1
0.3
0.6
1.0
Coupling Coefficient, β

Figure 3:

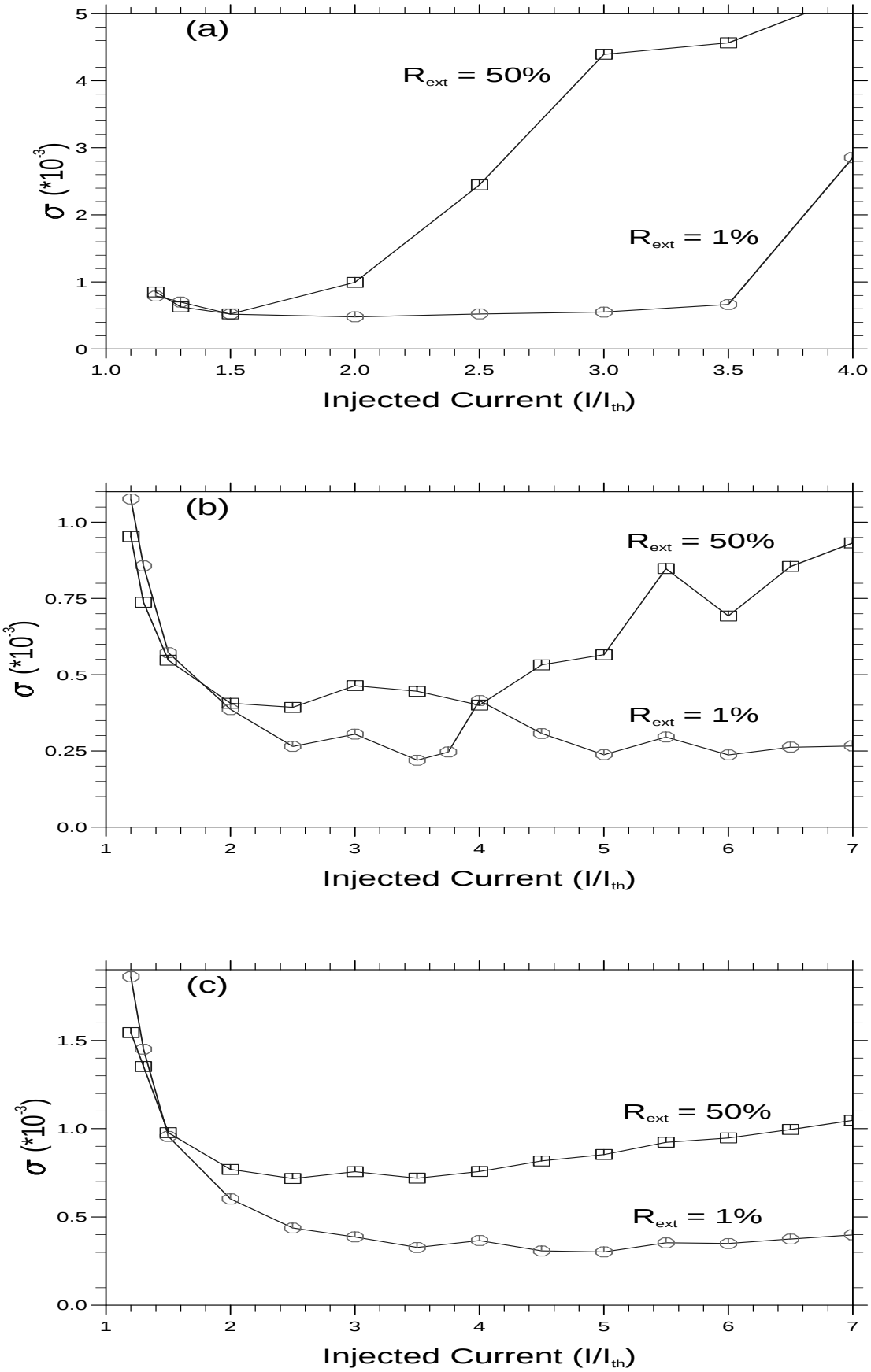
(a)
R_{ext} = 50%
R_{ext} = 1%
σ (*10^{-3})
Injected Current (I/I$_{th}$)
(b)
R_{ext} = 50%
R_{ext} = 1%
σ (*10^{-3})
Injected Current (I/I$_{th}$)
(c)
R_{ext} = 50%
R_{ext} = 1%
σ (*10^{-3})
Injected Current (I/I$_{th}$)

Figure 4:

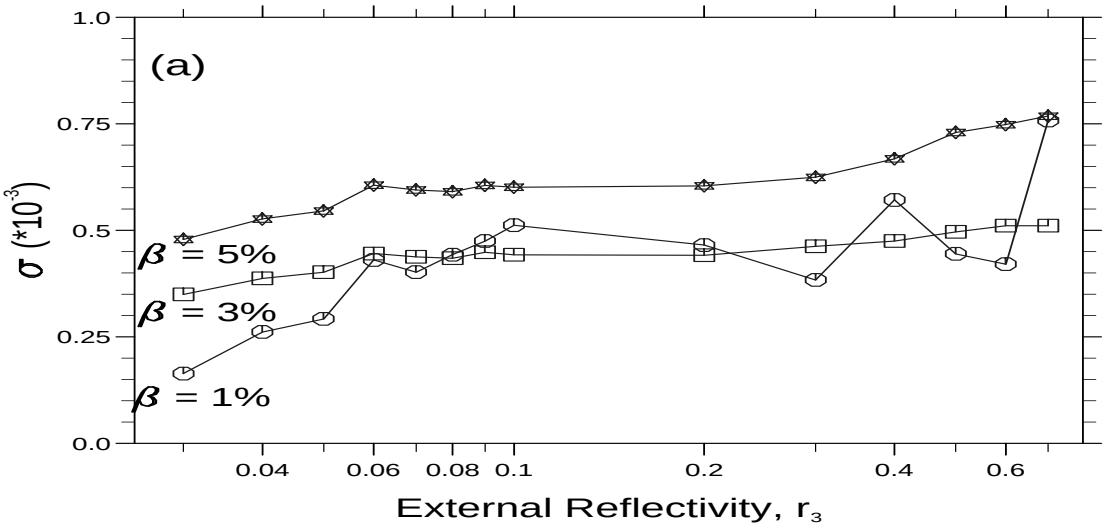
(a)
β = 5%
β = 3%
β = 1%
σ (*10^-3)
External Reflectivity, r3

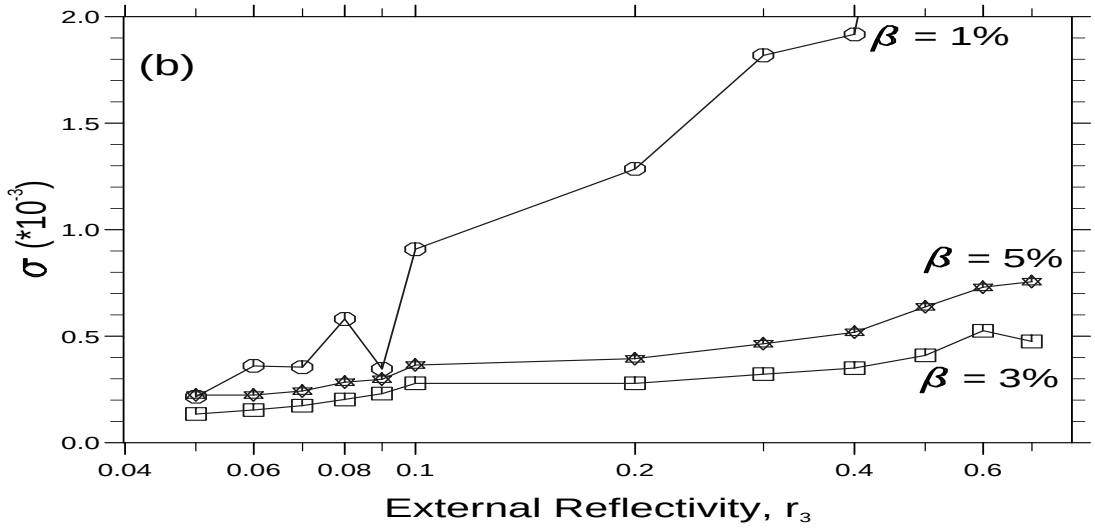
(b)
β = 1%
β = 5%
β = 3%
σ (*10^-3)
External Reflectivity, r3

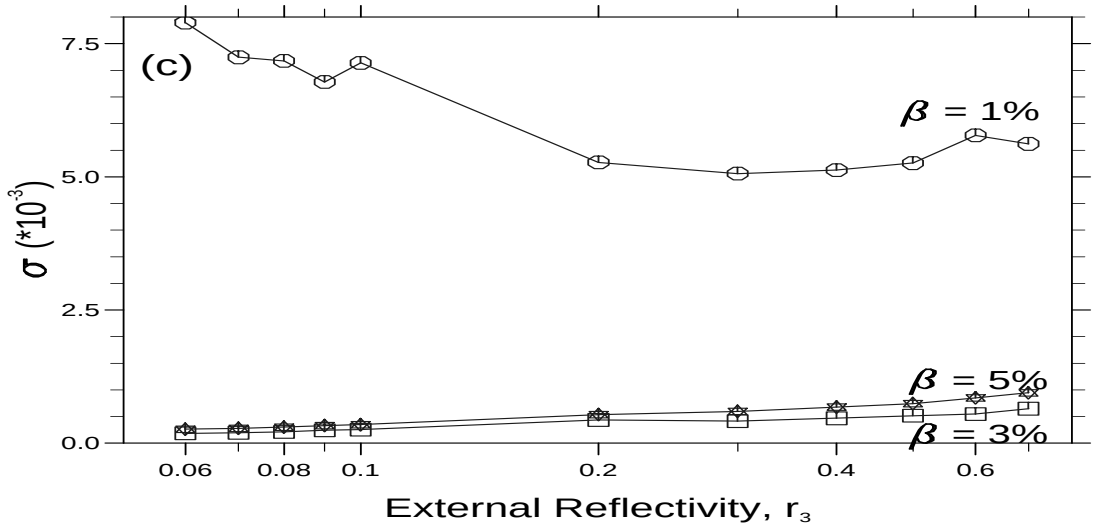
(c)
β = 1%
β = 5%
β = 3%
σ (*10^-3)
External Reflectivity, r3

Figure 5:

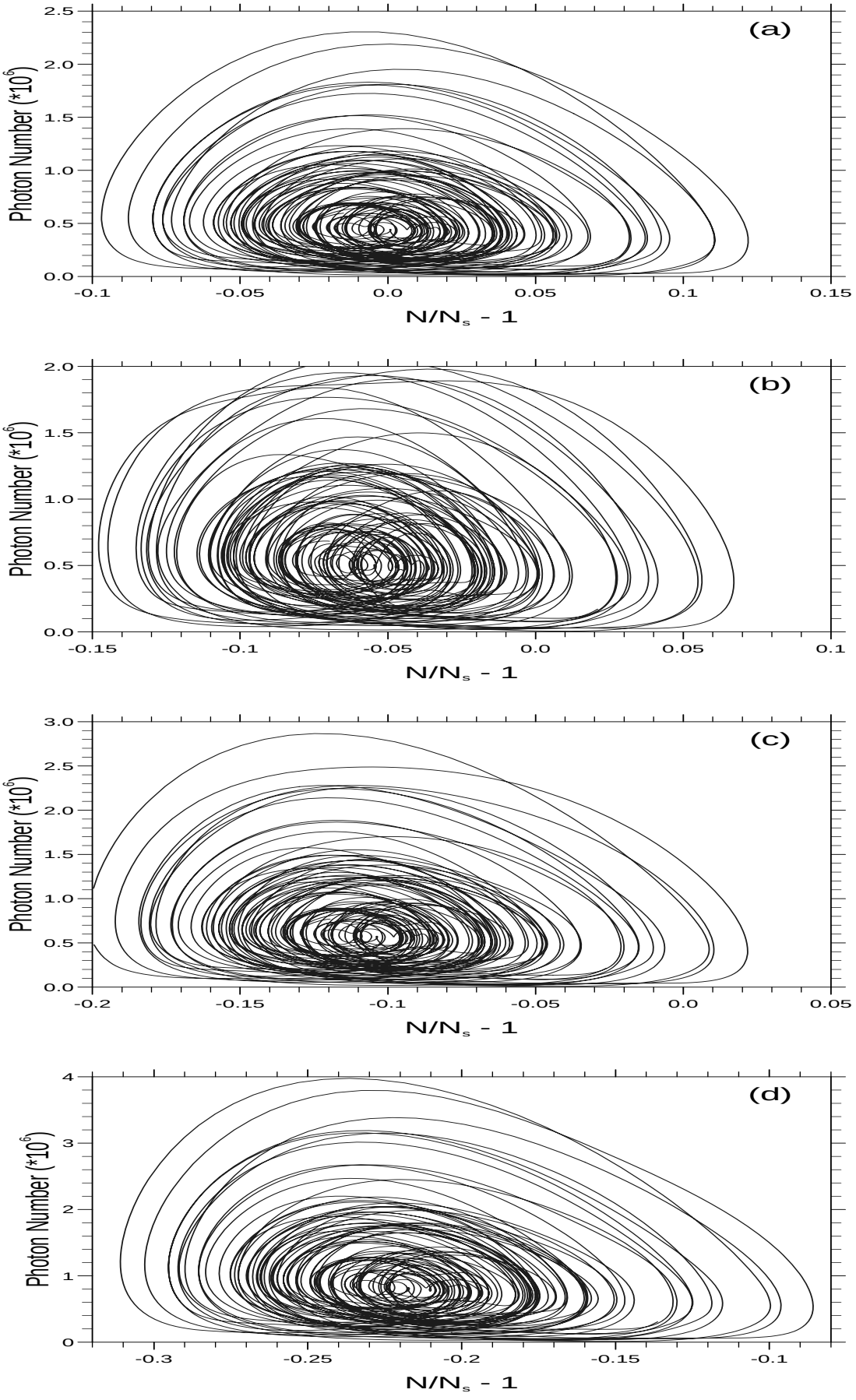
(a)
Photon Number (*10^6)
N/N_s - 1
(b)
Photon Number (*10^6)
N/N_s - 1
(c)
Photon Number (*10^6)
N/N_s - 1
(d)
Photon Number (*10^6)
N/N_s - 1

Figure 6:

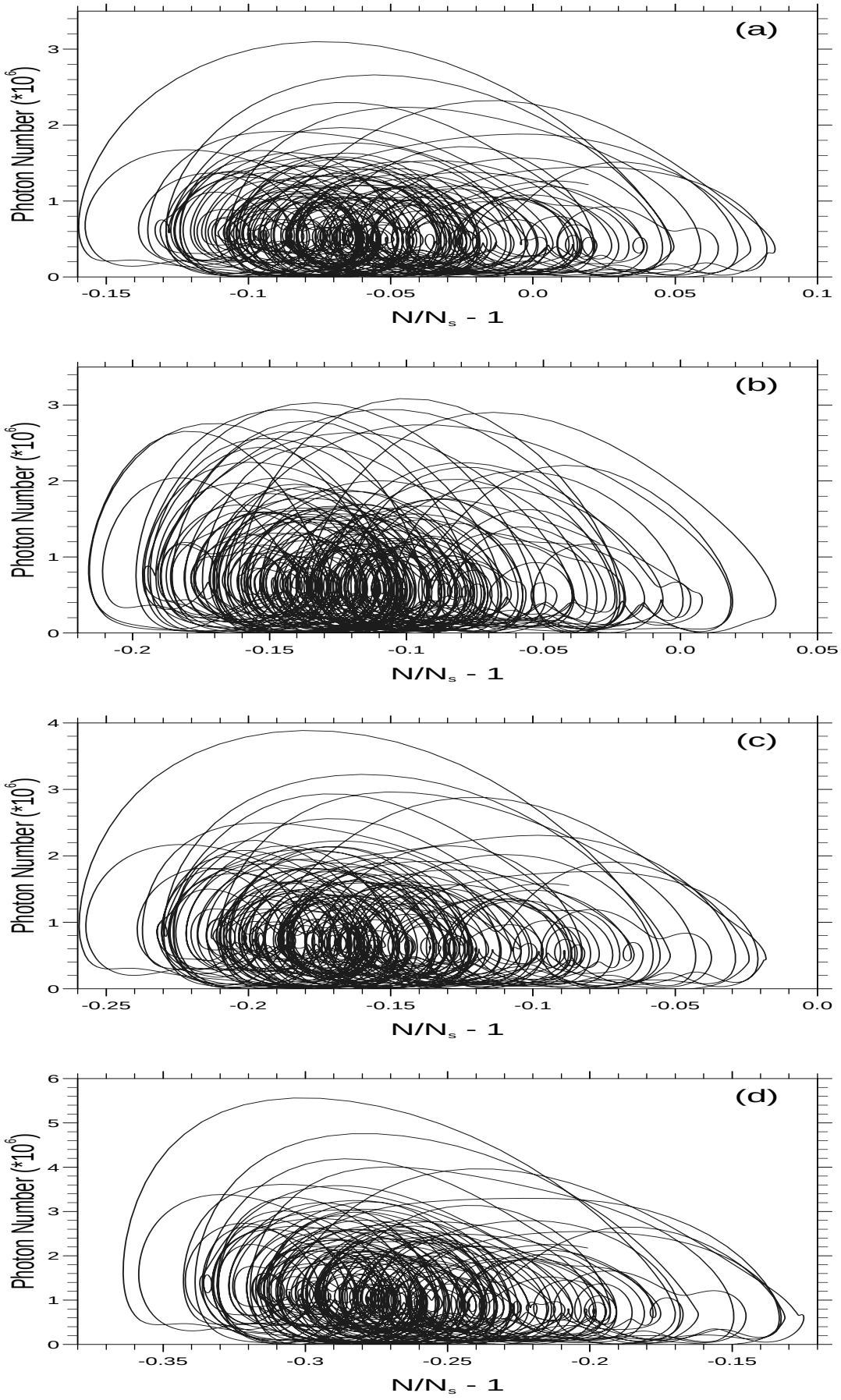
(a)
Photon Number (*10^6)
N/N_s - 1
(b)
Photon Number (*10^6)
N/N_s - 1
(c)
Photon Number (*10^6)
N/N_s - 1
(d)
Photon Number (*10^6)
N/N_s - 1

Figure 7: